JOURNAL OF MAGNETIC RESONANCE, Series A 109, 221–231 (1994)

Broadband, Narrowband, and Passband Composite Pulses for Use in Advanced NMR Experiments

STEPHEN WIMPERIS

Physical Chemistry Laboratory, University of Oxford, South Parks Road, Oxford OX1 3QZ, United Kingdom

Received December 1, 1993

New composite pulses are derived and presented in a simple form where the overall flip angle remains a variable. Thus, composite pulses of overall flip angle 45°, 90°, 135°, 180°, or, for example, 54.7°, can be written down in a matter of seconds. Composite pulses that, at exact resonance, exhibit either broadband, narrowband, or passband behavior with respect to the strength of the radiofrequency field are demonstrated. The performance of all these composite pulses remains satisfactory over a range of normalized resonance offsets typical of ^{1}H NMR spectroscopy. The most significant feature of the new composite pulses presented in this paper, however, is that they can be used to replace a simple pulse at any point in an advanced NMR experiment *without further modification of the pulse sequence.*

INTRODUCTION

The purpose of this paper is to present composite pulses (*1–18*) that can be used to replace a simple pulse at any point in an advanced NMR experiment, such as a NOESY or HMQC experiment, *without further modification of the pulse sequence.* These composite pulses are thus easier to use than other "phase distortionless" composite pulses (*4, 9, 12, 18*), many of which generate phase shifts that require later correction. The new composite pulses are derived and presented in a simple form where the overall flip angle remains a variable. Thus, if it is needed, a 54.7° or 120° composite pulse can be written down in a matter of seconds. In this paper, composite pulses of three basic types are demonstrated, namely those that, at exact resonance, exhibit broadband, narrowband, and passband (or "rectangular") behavior with respect to the strength of the radiofrequency field, B_1. Broadband composite pulses are the most widely used type as they can compensate for the deleterious effects of an inhomogeneous B_1 field, but narrowband or passband composite pulses can also be used in a number of more specialized applications. A further advantage of the broadband composite pulses presented in this paper is that, with respect to resonance offset Ω, they perform equally as well as the corresponding simple pulses.

DESIGN OF NEW COMPOSITE PULSES

The method used in this paper to design new composite pulses is an extension of that used previously to design composite pulses with passband (or rectangular) excitation and inversion profiles (*15*), broadband and narrowband excitation profiles (*16*), and broadband inversion profiles (*18*). Owing to this similarity, the following discussion will be kept as brief as possible. It should be emphasized, however, that these new composite pulses are designed with aims different from the design of the composite pulses of Refs. (*15, 16, 18*) and in no way supersede them. This section will start by deriving narrowband composite pulses, as the subsequent derivation of broadband and passband composite pulses will then be straightforward.

Narrowband Composite Pulses

Narrowband composite pulses excite or invert magnetization over only a narrow range of strengths of the radiofrequency field (*7, 8, 10, 16*). They have attracted interest as a possible means of exploiting the inevitable inhomogeneity of the B_1 field to obtain spatially localized NMR spectra *in vivo* (*19, 20*).

Consider a narrowband composite pulse consisting of four 180° pulses of arbitrary phase followed by a θ pulse of phase 0° (i.e., a pulse of flip angle θ degrees about the x axis of the rotating frame):

$$180^\circ_{\phi_1}180^\circ_{\phi_2}180^\circ_{\phi_3}180^\circ_{\phi_4}\theta_{0^\circ}. \qquad [1]$$

The advantages of starting from this *constrained form* (*15, 16, 18*) for the narrowband composite pulse will become clear in the course of this section. The flip angles given in Eq. [1] are the *nominal* flip angles. These are the flip angles associated with pulse durations, e.g., τ_{180° or τ_θ, that have been determined by assuming that the radiofrequency field strength, B_1, has a uniform, known value across the whole sample. In terms of these nominal flip angles, the propagator for the sequence in Eq. [1] applied to a single spin I at exact resonance, $\Omega = 0$, is given by

1064-1858/94 $6.00

$$U^{\text{nom}} = \exp\left\{-\frac{i\pi\theta}{180^\circ} I_x\right\}\exp\{-i\pi I_{\phi_4}\}\exp\{-i\pi I_{\phi_3}\} \times \exp\{-i\pi I_{\phi_2}\}\exp\{-i\pi I_{\phi_1}\}, \quad [2]$$

where $I_{\phi_j} = I_x\cos\phi_j + I_y\sin\phi_j$ and the phases ϕ_j are in degrees. After a simple rearrangement, this can be rewritten

$$U^{\text{nom}} = \exp\left\{-\frac{i\pi\theta}{180^\circ} I_x\right\}\exp\left\{\frac{2i\pi(\phi_1 - \phi_2 + \phi_3 - \phi_4)}{180^\circ} I_z\right\}. \quad [3]$$

The composite pulse in Eq. [1] is therefore nominally equivalent to a θ pulse about the rotating frame x axis *preceded* by a positive rotation about the rotating-frame z axis (or a phase shift) of $-2(\phi_1 - \phi_2 + \phi_3 - \phi_4)$ degrees. The aim of this paper is to derive composite pulses that, like simple pulses, do not generate this unwanted phase shift; hence the pulse phases, ϕ_1 to ϕ_4, will be chosen such that $-2(\phi_1 - \phi_2 + \phi_3 - \phi_4)$ is equal to zero.

In practice, there will never be a uniform radiofrequency field of known strength across the whole sample volume. Instead, there will be a continuous distribution of values of the nutation frequency, $\omega_1 = -\gamma B_1$. For example, in surface-coil experiments *in vivo,* the actual field strength in some parts of the "sample" may differ enormously from the nominal field strength, $B_1^{\text{nom}} = -\omega_1^{\text{nom}}/\gamma$, assumed when the pulse durations were determined. At exact resonance, the propagator for the sequence in Eq. [1] can be written for a single spin I and for arbitrary ω_1 as

$$U(\beta) = \exp\left\{-\frac{i\beta\theta}{180^\circ} I_x\right\}\exp\{-i\beta I_{\phi_4}\} \times \exp\{-i\beta I_{\phi_3}\}\exp\{-i\beta I_{\phi_2}\}\exp\{-i\beta I_{\phi_1}\}. \quad [4]$$

The actual flip angles of the pulses are here written in terms of a single variable $\beta = \omega_1\tau_{180^\circ}$ (i.e., the actual flip angle in radians produced by a nominal 180° pulse). In order to derive a narrowband composite pulse, the values of the phases ϕ_1 to ϕ_4 must be chosen such that $U(\beta) \approx \mathbb{1}$ for small values of β, where $\mathbb{1}$ is the identity operator. As a result of the desirable symmetry properties of the constrained form of the composite pulse in Eq. [1], this is sufficient to ensure narrowband behavior (*16*).

A first approach to setting $U(\beta) \approx \mathbb{1}$ for small values of β uses average Hamiltonian theory in the form pioneered by Tycko (*4*). The propagator $U(\beta)$ in Eq. [4] can be expanded as an infinite power series in the flip angle β:

$$U(\beta) = \exp\{-i\beta^{(0)}\mathbf{n}^{(0)}\cdot\mathbf{I} - i\beta^{(1)}\mathbf{n}^{(1)}\cdot\mathbf{I} - i\beta^{(2)}\mathbf{n}^{(2)}\cdot\mathbf{I} - \cdots\}. \quad [5]$$

General expressions for the zeroth-order average rotation $\beta^{(0)}\mathbf{n}^{(0)}\cdot\mathbf{I}$, the first-order average rotation $\beta^{(1)}\mathbf{n}^{(1)}\cdot\mathbf{I}$, and the second-order average rotation $\beta^{(2)}\mathbf{n}^{(2)}\cdot\mathbf{I}$ can be found elsewhere (*15*). For the special case of the constrained form of the composite pulse in Eq. [1], the zeroth- and first-order rotations reduce to the simple forms

$$\beta^{(0)}\mathbf{n}^{(0)}\cdot\mathbf{I} = \beta I_x\left(\cos\phi_1 + \cos\phi_2 + \cos\phi_3 + \cos\phi_4 + \frac{\theta}{180^\circ}\right) + \beta I_y(\sin\phi_1 + \sin\phi_2 + \sin\phi_3 + \sin\phi_4), \quad [6a]$$

$$\beta^{(1)}\mathbf{n}^{(1)}\cdot\mathbf{I} = \frac{\beta^2}{2} I_z\Big\{\sin(\phi_1 - \phi_2) + \sin(\phi_1 - \phi_3) + \sin(\phi_1 - \phi_4) + \sin(\phi_2 - \phi_3) + \sin(\phi_2 - \phi_4) + \sin(\phi_3 - \phi_4) + \frac{\theta}{180^\circ}(\sin\phi_1 + \sin\phi_2 + \sin\phi_3 + \sin\phi_4)\Big\}. \quad [6b]$$

The unit vectors $\mathbf{n}^{(0)}$ and $\mathbf{n}^{(1)}$ describe the rotation axes of the zeroth- and first-order average rotations, respectively. For very small β, only the zeroth-order rotation (which is linear in β) is significant and $U(\beta) \approx \exp\{-i\beta^{(0)}\mathbf{n}^{(0)}\cdot\mathbf{I}\}$. If the pulse phases ϕ_1 to ϕ_4 can be chosen such that $\beta^{(0)}\mathbf{n}^{(0)}\cdot\mathbf{I} = 0$, then $U(\beta) \approx \mathbb{1}$ for small values of β and a phase-distortionless narrowband composite pulse with flip angle θ will result. Such a goal has already been achieved in Ref. (*16*) with a much simpler composite pulse consisting of only two 180° pulses preceding a θ pulse. The advantage of using the extended constrained form of Eq. [1] is that it is now possible to set both the first-order average rotation $\beta^{(1)}\mathbf{n}^{(1)}\cdot\mathbf{I}$ and the unwanted $-2(\phi_1 - \phi_2 + \phi_3 - \phi_4)$ phase shift to zero. The approximation $U(\beta) \approx \exp\{-i\beta^{(0)}\mathbf{n}^{(0)}\cdot\mathbf{I} - i\beta^{(1)}\mathbf{n}^{(1)}\cdot\mathbf{I}\}$ holds over a wider range of values of β than the simple zeroth-order approximation and, if the phases ϕ_1 to ϕ_4 can be chosen such that $\beta^{(0)}\mathbf{n}^{(0)}\cdot\mathbf{I} = \beta^{(1)}\mathbf{n}^{(1)}\cdot\mathbf{I} = 0$, then a narrowband composite pulse with superior performance will result.

With the freedom provided by four phases, ϕ_1 to ϕ_4, it is a simple matter to set the zeroth-order rotation to zero. If it is assumed that $\beta^{(0)}\mathbf{n}^{(0)}\cdot\mathbf{I} = 0$, the first-order average rotation in Eq. [6b] reduces to

$$\beta^{(1)}\mathbf{n}^{(1)}\cdot\mathbf{I} = \frac{\beta^2}{2} I_z\{\sin(\phi_1 - \phi_2) + \sin(\phi_1 - \phi_3) + \sin(\phi_1 - \phi_4) + \sin(\phi_2 - \phi_3) + \sin(\phi_2 - \phi_4) + \sin(\phi_3 - \phi_4)\}. \quad [7]$$

By inspection, this term can easily be set to zero by choosing $\phi_1 = \phi_4$ and $\phi_2 = \phi_3$. This is not the only way of achieving $\beta^{(1)}\mathbf{n}^{(1)}\cdot\mathbf{I} = 0$, but it has the obvious advantage that the unwanted phase shift of $-2(\phi_1 - \phi_2 + \phi_3 - \phi_4)$ also becomes zero. With these constraints, the zeroth-order rotation in Eq. [6a] becomes

$$\beta^{(0)}\mathbf{n}^{(0)} \cdot \mathbf{I} = 2\beta I_x\left(\cos\phi_1 + \cos\phi_2 + \frac{\theta}{360°}\right) + 2\beta I_y(\sin\phi_1 + \sin\phi_2). \quad [8]$$

The equation $\beta^{(0)}\mathbf{n}^{(0)} \cdot \mathbf{I} = 0$ is now easily solved with the phases $\phi_1 = \cos^{-1}(-\theta/720°)$ and $\phi_2 = -\phi_1$. Thus a general form for a θ composite pulse which is narrowband to first order and which can be used to replace a simple θ pulse about the x axis can be given as

$$\mathrm{NB}_1(\theta): 180°_{\phi_1}360°_{\phi_2}180°_{\phi_1}\theta_{0°}, \quad [9]$$

with $\phi_1 = \cos^{-1}(-\theta/720°)$ and $\phi_2 = -\phi_1$.

An alternative approach to ensuring that $U(\beta) \approx \mathbb{1}$ for small values of β (*8, 15, 16, 18*) consists of using intuitive rotation-operator arguments to find values for the phases ϕ_1 to ϕ_4 such that $U(\beta = \pi/2) = \mathbb{1}$. Since $U(\beta = 0) = \mathbb{1}$ by definition, it can then be assumed that $U(\beta) = \mathbb{1}$ for all values of β between 0 and $\pi/2$. As before, the pulse phases ϕ_1 to ϕ_4 must also be chosen such that $-2(\phi_1 - \phi_2 + \phi_3 - \phi_4) = 0$. These two conditions can be met by having $\phi_1 = \phi_4 = 90°$ and $\phi_2 = \phi_3 = 270° - \theta/4$. Thus, an alternative form for a narrowband θ composite pulse which can be used to replace a simple θ pulse about the x axis can be given as

$$\mathrm{NB}_2(\theta): 180°_{90°}360°_{\phi_2}180°_{90°}\theta_{0°}, \quad [10]$$

with $\phi_2 = 270° - \theta/4$.

The composite pulses $\mathrm{NB}_1(\theta)$ and $\mathrm{NB}_2(\theta)$ that emerge from Eqs. [9] and [10] for overall flip angles of $\theta = 45°$, 90°, 135°, and 180° are given in Table 1. The simulated excitation or inversion profiles of the narrowband composite 90° and 180° pulses are compared to those of the corresponding simple pulses as function of the normalized radiofrequency field, $\omega_1/\omega_1^{\mathrm{nom}}$, in Fig. 1. In Figs. 1a and 1c the composite pulses are applied to an initial state $\sigma(0) = I_z$ and in Figs. 1b and 1d to $\sigma(0) = I_y$. Two profiles, showing either the resulting expectation value of longitudinal magnetization, $\langle I_z \rangle$, or absorptive magnetization, $\langle I_y \rangle$, are simulated for each composite pulse. The narrowband performance and absence of significant phase distortion can be seen.

TABLE 1

Narrowband, Broadband, and Passband Composite Pulses with Overall Flip Angles $\theta = 45°$, 90°, 135°, and 180°

Narrowband composite pulses	NB_1 (45°)	$180°_{93.6°}360°_{266.4°}180°_{93.6°}45°_{0°}$
	NB_1 (90°)	$180°_{97.2°}360°_{262.8°}180°_{97.2°}90°_{0°}$
	NB_1 (135°)	$180°_{100.8°}360°_{259.2°}180°_{100.8°}135°_{0°}$
	NB_1 (180°)	$180°_{104.5°}360°_{255.5°}180°_{104.5°}180°_{0°}$
	NB_2 (45°)	$180°_{90°}360°_{258.75°}180°_{90°}45°_{0°}$
	NB_2 (90°)	$180°_{90°}360°_{247.5°}180°_{90°}90°_{0°}$
	NB_2 (135°)	$180°_{90°}360°_{236.25°}180°_{90°}135°_{0°}$
	NB_2 (180°)	$180°_{90°}360°_{225°}180°_{90°}180°_{0°}$
Broadband composite pulses	BB_1 (45°)	$180°_{93.6°}360°_{280.7°}180°_{93.6°}45°_{0°}$
	BB_1 (90°)	$180°_{97.2°}360°_{91.5°}180°_{97.2°}90°_{0°}$
	BB_1 (135°)	$180°_{100.8°}360°_{302.4°}180°_{100.8°}135°_{0°}$
	BB_1 (180°)	$180°_{104.5°}360°_{313.4°}180°_{104.5°}180°_{0°}$
	BB_2 (45°)	$180°_{90°}360°_{281.25°}180°_{90°}45°_{0°}$
	BB_2 (90°)	$180°_{90°}360°_{292.5°}180°_{90°}90°_{0°}$
	BB_2 (135°)	$180°_{90°}360°_{303.75°}180°_{90°}135°_{0°}$
	BB_2 (180°)	$180°_{90°}360°_{315°}180°_{90°}180°_{0°}$
Passband composite pulses	PB_1 (45°)	$360°_{91.8°}720°_{268.2°}360°_{91.8°}45°_{0°}$
	PB_1 (90°)	$360°_{93.6°}720°_{266.4°}360°_{93.6°}90°_{0°}$
	PB_1 (135°)	$360°_{95.3°}720°_{264.6°}360°_{95.3°}135°_{0°}$
	PB_1 (180°)	$360°_{97.2°}720°_{262.8°}360°_{97.2°}180°_{0°}$
	PB_2 (45°)	$360°_{90°}720°_{264.375°}360°_{90°}45°_{0°}$
	PB_2 (90°)	$360°_{90°}720°_{258.75°}360°_{90°}90°_{0°}$
	PB_2 (135°)	$360°_{90°}720°_{253.125°}360°_{90°}135°_{0°}$
	PB_2 (180°)	$360°_{90°}720°_{247.5°}360°_{90°}180°_{0°}$

Broadband Composite Pulses

Broadband composite pulses excite or invert magnetization over a broader range of radiofrequency field strengths than a simple pulse (*1–10, 14, 16*). They have therefore been widely used to compensate for the deleterious effects of inhomogeneous B_1 radiofrequency fields in high-resolution NMR experiments.

The constrained form of composite pulse given in Eq. [1] is also appropriate to the design of broadband composite pulses. When used as a broadband pulse, such a sequence is, of course, still nominally equivalent to a θ pulse about the x axis preceded by a phase shift of $-2(\phi_1 - \phi_2 + \phi_3 - \phi_4)$. The propagator for the sequence in Eq. [1] is given by Eq. [4] but here this propagator is split into two parts:

$$U(\beta) = U^{\mathrm{nom}}\tilde{U}(\delta), \quad [11]$$

where U^{nom} is given by Eq. [2]. If, for the moment, it is assumed that $-2(\phi_1 - \phi_2 + \phi_3 - \phi_4) = 0$, the propagator $\tilde{U}(\delta)$ takes the simple form

$$\tilde{U}(\delta) = \exp\left\{-\frac{i\delta\theta}{180°}I_x\right\}\exp\{-i\delta I_{\phi_4'}\} \times \exp\{-i\delta I_{\phi_3'}\}\exp\{-i\delta I_{\phi_2'}\}\exp\{-i\delta I_{\phi_1'}\}, \quad [12]$$

where $\delta = \beta - \pi = (\omega_1 - \omega_1^{\mathrm{nom}})\tau_{180°}$ and the "toggling-frame" phases (*16, 18*) are given by

$$\phi_j' = -(-1)^j\phi_j - \sum_{k=1}^{j-1}(-1)^k 2\phi_k. \quad [13]$$

In order to achieve broadband behavior, the values of the toggling-frame phases ϕ_1' to ϕ_4' must be chosen such that $\tilde{U}(\delta) \approx \mathbb{1}$ for small values of δ. Then, over the same range of δ, the propagator $U(\beta) \approx U^{\mathrm{nom}}$ and a phase-distortionless broadband composite pulse with flip angle θ will result. The propagator $\tilde{U}(\delta)$ in Eq. [12] can be expanded as an infinite power series in the flip angle δ in a precisely analogous fashion to Eq. [5]. The zeroth- and first-order average rotations $\delta^{(0)}\mathbf{n}^{(0)} \cdot \mathbf{I}$ and $\delta^{(1)}\mathbf{n}^{(1)} \cdot \mathbf{I}$ are given by Eqs. [6a] and [6b]

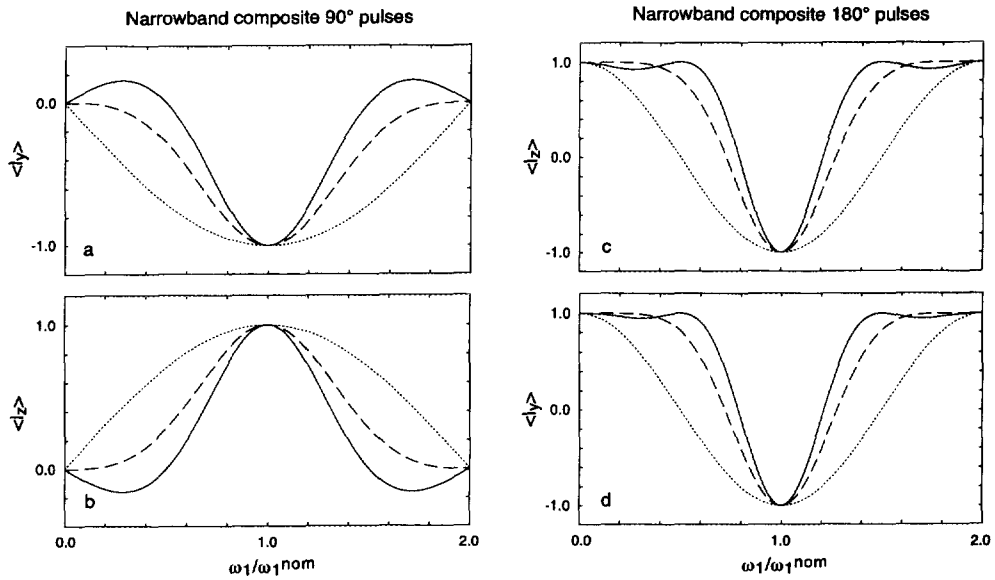

FIG. 1. Simulated performance at exact resonance ($\Omega = 0$) of (a, b) the narrowband composite 90° pulses $NB_1(90°)$ and $NB_2(90°)$ and (c, d) the narrowband composite 180° pulses $NB_1(180°)$ and $NB_2(180°)$ as a function of the normalized B_1 field strength, ω_1/ω_1^{nom}. The excitation profiles in (a) show the expectation value of absorptive magnetization, $\langle I_y \rangle$, excited by a simple 90°_0 pulse (dotted line) and the composite 90° pulses $NB_1(90°)$ (dashed line) and $NB_2(90°)$ (solid line) when applied to an initial state $\sigma(0) = I_z$. The profiles in (b) are similar, except that they show the expectation value of longitudinal magnetization, $\langle I_z \rangle$, created by the simple and narrowband composite 90° pulses when applied to an initial state $\sigma(0) = I_y$. The inversion profiles in (c) show the longitudinal magnetization, $\langle I_z \rangle$, created by a simple 180°_0 pulse (dotted line) and the composite 180° pulses $NB_1(180°)$ (dashed line) and $NB_2(180°)$ (solid line) when applied to an initial state $\sigma(0) = I_z$. The profiles in (d) are similar, except that they show the absorptive magnetization, $\langle I_y \rangle$, created by the simple and narrowband composite 180° pulses when applied to an initial state $\sigma(0) = I_y$.

except that β is replaced by δ and the pulse phases ϕ_j are replaced by the toggling-frame phases ϕ'_j. One way of achieving the condition $\delta^{(0)}\mathbf{n}^{(0)} \cdot \mathbf{I} = \delta^{(1)}\mathbf{n}^{(1)} \cdot \mathbf{I} = 0$ is therefore to have $\phi'_1 = \phi'_4$ and $\phi'_2 = \phi'_3$ and to have $\phi'_1 = \cos^{-1}(-\theta/720°)$ and $\phi'_2 = -\phi'_1$ in precise analogy to the result for narrowband composite pulses. The actual pulse phases ϕ_1 to ϕ_4 can be calculated from Eq. [13] and emerge as $\phi_1 = \phi_4$ and $\phi_2 = \phi_3$ and $\phi_1 = \cos^{-1}(-\theta/720°)$ and $\phi_2 = 3\phi_1$. Thus, the unwanted phase shift of $-2(\phi_1 - \phi_2 + \phi_3 - \phi_4)$ is again zero. A general form for a θ composite pulse which is broadband to first order and which can be used to replace a simple θ pulse about the x axis can therefore be given as

$$BB_1(\theta)\text{: } 180^\circ_{\phi_1}360^\circ_{\phi_2}180^\circ_{\phi_1}\theta_{0°}, \qquad [14]$$

with $\phi_1 = \cos^{-1}(-\theta/720°)$ and $\phi_2 = 3\phi_1$.

As with the narrowband composite pulses, an alternative approach to ensuring that $\tilde{U}(\delta) \approx \mathbb{1}$ for small values of δ is to find values for the toggling-frame phases ϕ'_1 to ϕ'_4 such that $\tilde{U}(\delta = \pi/2) = \mathbb{1}$. It can then be assumed that $U(\beta) \approx U^{nom}$ for all values of β between $\pi/2$ and π. As before, suitable phases can be derived immediately from the relevant narrowband case as $\phi'_1 = \phi'_4 = 90°$ and $\phi'_2 = \phi'_3 = 270° - \theta/4$. The corresponding pulse phases are $\phi_1 = \phi_4 = 90°$ and $\phi_2 = \phi_3 = 270° + \theta/4$. Note that the unwanted phase shift of $-2(\phi_1 - \phi_2 + \phi_3 - \phi_4)$ is again zero. Thus an alternative form for a broadband θ composite pulse which can be used to replace a simple θ pulse about the x axis can be given as

$$BB_2(\theta)\text{: } 180^\circ_{90°}360^\circ_{\phi_2}180^\circ_{90°}\theta_{0°}, \qquad [15]$$

with $\phi_2 = 270° + \theta/4$.

Table 1 lists the broadband composite pulses $BB_1(\theta)$ and $BB_2(\theta)$ that emerge from Eqs. [14] and [15] for overall flip angles of $\theta = 45°$, 90°, 135°, and 180°. Figure 2 compares (in the same format as Fig. 1) the simulated excitation or inversion profiles of the broadband composite 90° pulse and 180° pulses to those of the corresponding simple pulses at exact resonance, $\Omega = 0$. Note that the $BB_2(\theta)$ composite pulses yield broader bandwidths than the $BB_1(\theta)$ pulses but are slightly less accurate within these bandwidths. The absence of significant phase distortion is apparent for both the $BB_1(\theta)$ and the $BB_2(\theta)$ composite pulses.

Passband Composite Pulses

Passband or rectangular-profile composite pulses exhibit both narrowband and broadband behavior simultaneously (*11, 13, 15*). As with narrowband composite pulses, they are chiefly of interest as a method of obtaining spatially localized NMR spectra in the presence of inhomogeneous B_1 fields.

The constrained form of passband composite pulse used in this paper consists of four nominal 360° pulses of arbitrary phase followed by a θ pulse of phase 0°:

$$360^\circ_{\phi_1}360^\circ_{\phi_2}360^\circ_{\phi_3}360^\circ_{\phi_4}\theta_{0°}. \qquad [16]$$

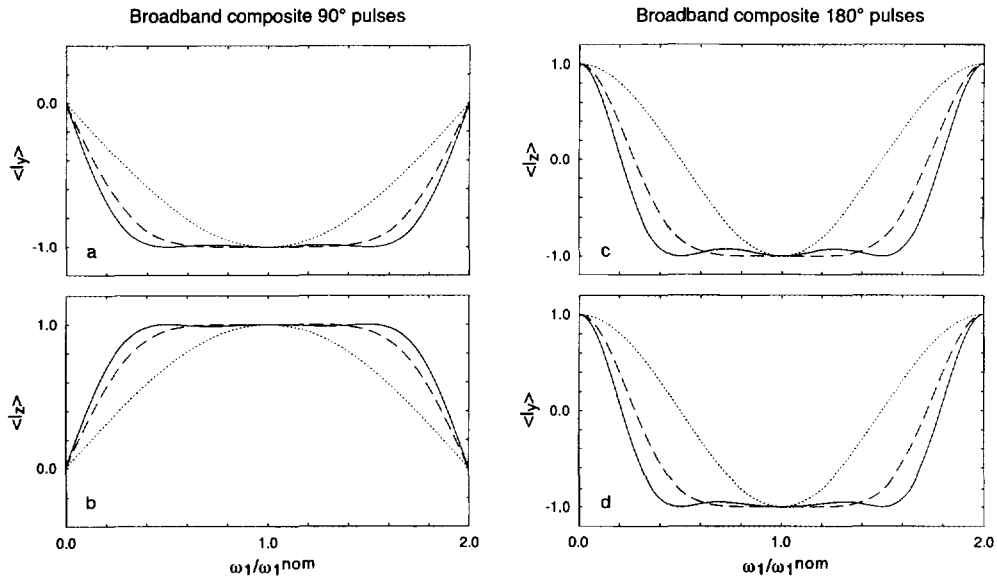

FIG. 2. Simulated performance at exact resonance ($\Omega = 0$) of (a, b) the broadband composite 90° pulses $BB_1(90°)$ (dashed lines) and $BB_2(90°)$ (solid lines) and (c, d) the broadband composite 180° pulses $BB_1(180°)$ (dashed lines) and $BB_2(180°)$ (solid lines) as a function of the normalized B_1 field strength, ω_1/ω_1^{nom}. The excitation or inversion profiles of a simple 90°_0 pulse in (a, b) and a simple 180°_0 pulse in (c, d) are shown as dotted lines. The plots in (a–d) show the same magnetizations and are for the same initial states as given in the legend to Fig. 1.

The exponential operator describing a 360° pulse, $\exp\{-i2\pi I_{\phi_j}\}$, is equal to the identity operator, $\mathbb{1}$. Thus, the nominal propagator for the sequence in Eq. [16] applied to a single spin I at exact resonance, $\Omega = 0$, is simply

$$U^{nom} = \exp\left\{-\frac{i\pi\theta}{180°} I_x\right\}. \qquad [17]$$

For this constrained form of composite pulse, there is therefore no unwanted phase shift, whatever the values of the pulse phases ϕ_1 to ϕ_4. The advantage of this constrained form is that the propagator analogous to Eq. [4] can be written

$$U(\beta) = \exp\left\{-\frac{i\beta\theta}{180°} I_x\right\}\exp\{-i2\beta I_{\phi_4}\}\exp\{-i2\beta I_{\phi_3}\} \times \exp\{-i2\beta I_{\phi_2}\}\exp\{-i2\beta I_{\phi_1}\}, \qquad [18]$$

where β is again the actual flip angle of a nominal 180° pulse, while the toggling-frame propagator analogous to Eq. [12] can be written

$$\tilde{U}(\delta) = \exp\left\{-\frac{i\delta\theta}{180°} I_x\right\}\exp\{-i2\delta I_{\phi_4}\}\exp\{-i2\delta I_{\phi_3}\} \times \exp\{-i2\delta I_{\phi_2}\}\exp\{-i2\delta I_{\phi_1}\}, \qquad [19]$$

where $\delta = \beta - \pi$ again. Note that the phases in $\tilde{U}(\delta)$ in Eq. [19] are the actual pulse phases ϕ_1 to ϕ_4. It can be seen that $U(\beta)$ and $\tilde{U}(\delta)$ are identical apart from the trivial change of variable. Thus, if average-Hamiltonian or rotation-operator methods are used to set $U(\beta) \approx \mathbb{1}$ for small β, then $\tilde{U}(\delta) \approx \mathbb{1}$ for the same composite pulse (*15*). This represents the presence of broadband and narrowband behavior simultaneously, hence passband behavior. Since all that must be done is to set $U(\beta) \approx \mathbb{1}$ for small β, it is possible to proceed directly from the results for narrowband composite pulses to the following results for passband θ composite pulses which can be used to replace a simple θ pulse about the x axis. The passband composite pulses obtained from average-Hamiltonian theory are given by

$$PB_1(\theta)\text{: } 360^\circ_{\phi_1}720^\circ_{\phi_2}360^\circ_{\phi_1}\theta_{0^\circ}, \qquad [20]$$

with $\phi_1 = \cos^{-1}(-\theta/1440°)$ and $\phi_2 = -\phi_1$, while the alternative passband composite pulses obtained from rotation operator arguments are given by

$$PB_2(\theta)\text{: } 360^\circ_{90^\circ}720^\circ_{\phi_2}360^\circ_{90^\circ}\theta_{0^\circ}, \qquad [21]$$

with $\phi_2 = 270° - \theta/8$.

The passband composite pulses $PB_1(\theta)$ and $PB_2(\theta)$ that emerge from Eqs. [20] and [21] for overall flip angles of $\theta = 45°$, 90°, 135°, and 180° are given in Table 1. Figure 3 compares (in the same format as Fig. 1) the simulated excitation or inversion profiles of the passband composite 90° pulse and 180° pulses as a function of ω_1/ω_1^{nom} to those of the corresponding simple pulses at exact resonance, $\Omega = 0$.

PERFORMANCE AT NONZERO RESONANCE OFFSETS

A typical ^1H NMR spectrum of a liquid sample recorded at 600 MHz usually has, at most, a 6 kHz spread of resonance

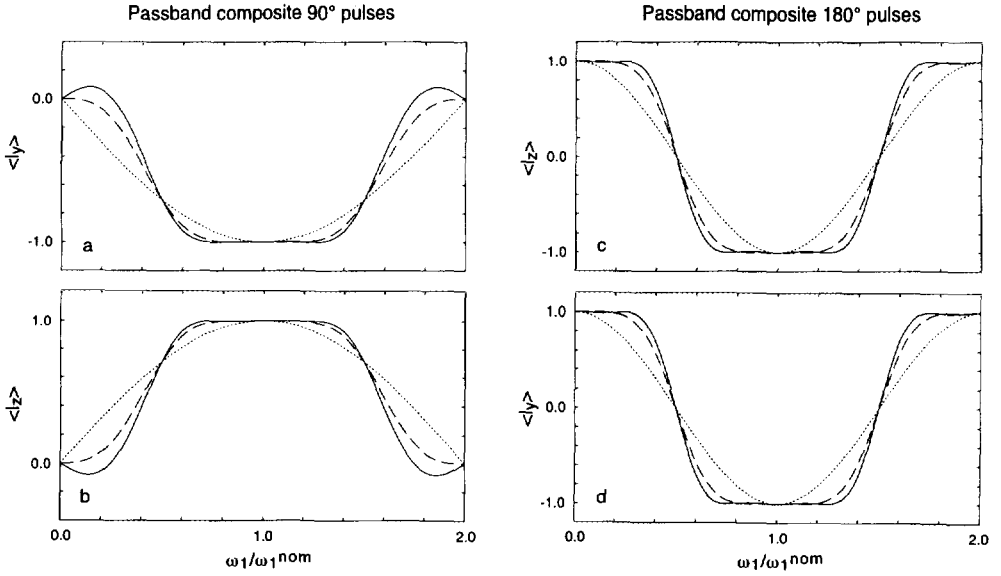

FIG. 3. Simulated performance at exact resonance ($\Omega = 0$) of (a, b) the passband composite 90° pulses $PB_1(90°)$ (dashed lines) and $PB_2(90°)$ (solid lines) and (c, d) the passband composite 180° pulses $PB_1(180°)$ (dashed lines) and $PB_2(180°)$ (solid lines) as a function of the normalized B_1 field strength, ω_1/ω_1^{nom}. The excitation or inversion profiles of a simple $90^\circ_{0^\circ}$ pulse in (a, b) and a simple $180^\circ_{0^\circ}$ pulse in (c, d) are shown as dotted lines. The plots in (a–d) show the same magnetizations and are for the same initial states as given in the legend to Fig. 1.

frequencies. If the transmitter is placed in the center of the spectrum, the maximum offset from resonance is $\Omega/2\pi = \pm 3$ kHz. A typical ^{1}H 90° pulse length on a 600 MHz NMR spectrometer is ~ 7 μs, corresponding to a nutation frequency of $\omega_1^{nom}/2\pi = 35.7$ kHz. Therefore, the maximum normalized offset, Ω/ω_1^{nom}, likely to occur in ^{1}H spectroscopy of liquids is ±0.084. The broadband, narrowband, and passband composite pulses presented in the previous section have all been derived given the assumption that the transmitter is placed on exact resonance, $\Omega = 0$. The above estimate shows, however, that if these pulses are to prove useful in routine ^{1}H spectroscopy, they will have to be effective over the range of resonance offsets $-0.1 \leq \Omega/\omega_1^{nom} \leq 0.1$. This is approximately the offset range over which a simple 90° or 180°

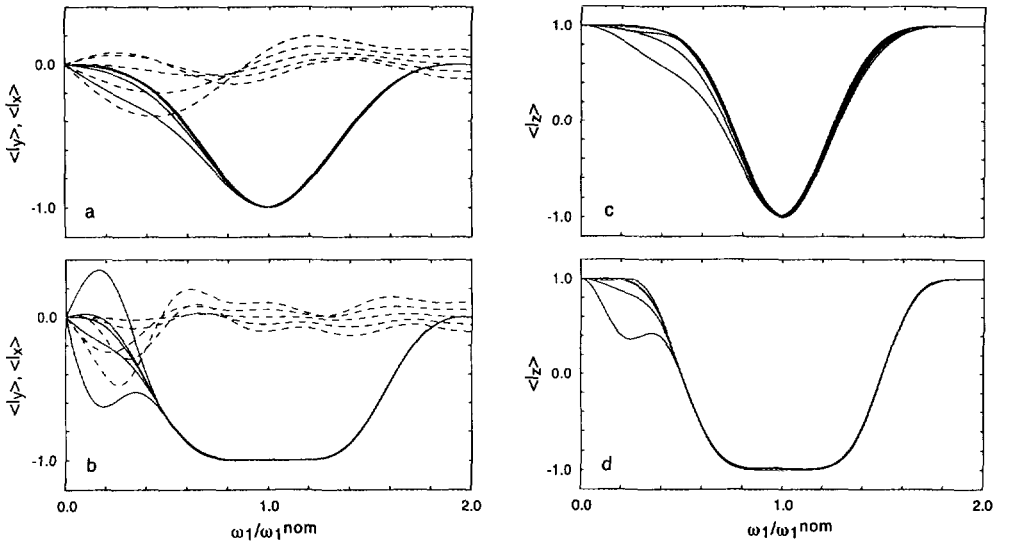

FIG. 4. Simulated performance of narrowband and passband composite 90° and 180° pulses at nonzero resonance offsets. Excitation or inversion profiles of the composite pulses (a) $NB_1(90°)$, (b) $PB_1(90°)$, (c) $NB_1(180°)$, and (d) $PB_1(180°)$ as a function of ω_1/ω_1^{nom} are shown superimposed for the five values of the normalized resonance offset, $\Omega/\omega_1^{nom} = -0.1, -0.05, 0.0, 0.05$, and 0.1. For the 90° pulses in (a) and (b), both the absorptive, $\langle I_y \rangle$ (solid lines), and the dispersive, $\langle I_x \rangle$ (dashed lines), excitation profiles are shown, while just the inversion profiles, $\langle I_z \rangle$, are shown in (c) and (d). The initial state is $\sigma(0) = I_z$ for all profiles.

pulse works well. However, most composite pulses designed for use with inhomogeneous B_1 fields are effective only over a much smaller range of offsets than this.

In a similar fashion to the previous section, average-Hamiltonian theory has also been used to design composite pulses that are broadband with respect to resonance offset (*4, 9, 21*). A well-known result is that a simple 360° pulse is broadband to zeroth order with respect to resonance offset, Ω. In consequence, a simple, nominal 360° pulse performs essentially perfectly over the fairly wide range of normalized offsets $-0.2 \leq \Omega/\omega_1^{nom} \leq 0.2$. The passband composite pulses $PB_1(\theta)$ and $PB_2(\theta)$ in Eqs. [20] and [21] consist of a series of 360° pulses followed by a θ pulse. (A 720° pulse is just two successive 360° pulses with the same phase!) Therefore, *to zeroth order*, the performance of the passband composite pulses with respect to resonance offset is predicted to be identical to that of the θ pulses that they are designed to replace. Similarly, it can easily be shown that a sequence of three pulses of the form $180^\circ_{\phi_1}360^\circ_{\phi_2}180^\circ_{\phi_1}$ (with arbitrary values of ϕ_1 and ϕ_2) is broadband to zeroth order with respect to resonance offset. Thus, the narrowband composite pulses $NB_1(\theta)$ and $NB_2(\theta)$ in Eqs. [9] and [10] and the broadband composite pulses $BB_1(\theta)$ and $BB_2(\theta)$ in Eqs. [14] and [15] are also predicted to perform no worse at small resonance offsets than the simple θ pulses that they are designed to replace.

The performance of narrowband and passband composite 90° and 180° pulses over a range of resonance offsets is simulated in Fig. 4. The excitation or inversion profiles of the composite pulses (Fig. 4a) $NB_1(90°)$, (Fig. 4b) $PB_1(90°)$, (Fig. 4c) $NB_1(180°)$, and (Fig. 4d) $PB_1(180°)$ as a function of ω_1/ω_1^{nom} for the five values of the normalized resonance offset, $\Omega/\omega_1^{nom} = -0.1, -0.05, 0.0, 0.05$, and 0.1, are shown superimposed. For the 90° pulses in Figs. 4a and 4b, both the absorptive, $\langle I_y \rangle$, and the dispersive, $\langle I_x \rangle$, excitation profiles are shown, while just the inversion profiles, $\langle I_z \rangle$, are shown in Figs. 4c and 4d for the 180° pulses. As predicted

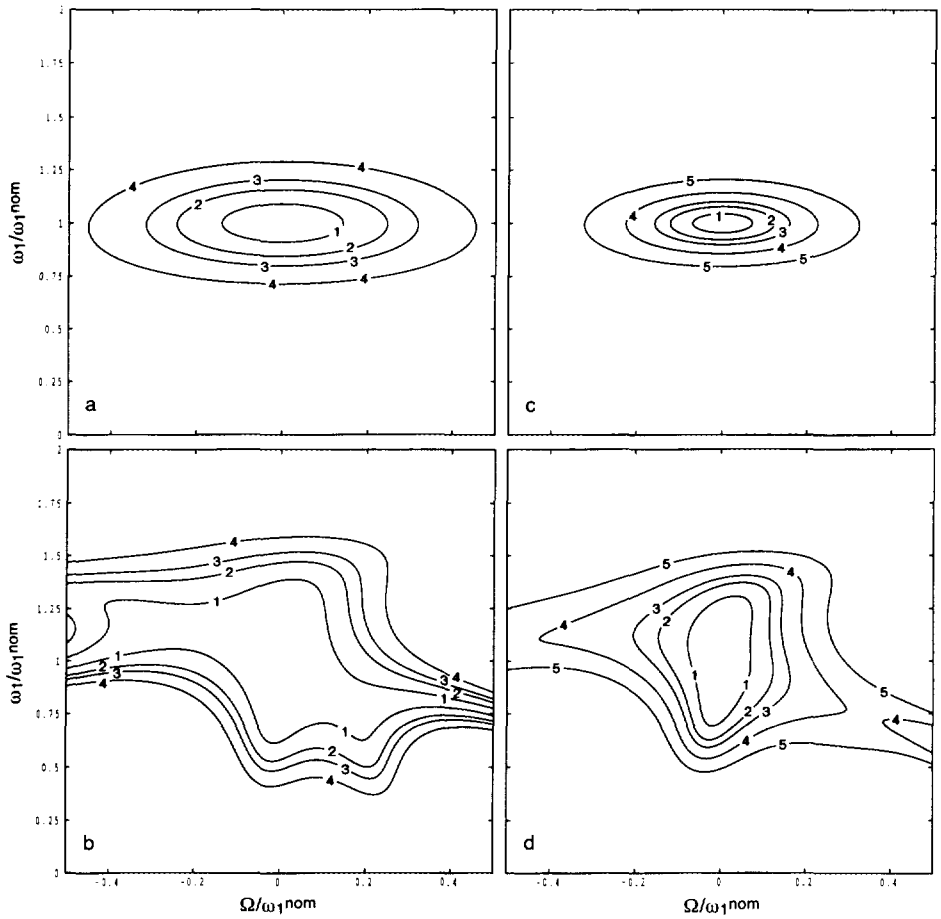

FIG. 5. Simulated performance of simple and broadband composite 90° and 180° pulses over a range of resonance offsets. Contour plots show the extent of excitation or inversion with the normalized resonance offset on the horizontal axis ($-0.5 \leq \Omega/\omega_1^{nom} \leq +0.5$) and the normalized B_1 field strength on the vertical axis ($0 \leq \omega_1/\omega_1^{nom} \leq 2$). Contour plots (a) and (b) show the absorptive excitation, $\langle I_y \rangle$, for a simple 90°_0 pulse and the broadband composite 90° pulse $BB_1(90°)$, while (c) and (d) show the inversion, $\langle I_z \rangle$, for a simple 180°_0 pulse and the broadband composite 180° pulse $BB_1(180°)$. In (a) and (b) contours are drawn at (1) $\langle I_y \rangle = -0.99$, (2) −0.97, (3) −0.95, and (4) −0.90, while in (c) and (d) they are drawn at (1) $\langle I_z \rangle = -0.99$, (2) −0.97, (3) −0.95, (4) −0.90, and (5) −0.80. The initial state is $\sigma(0) = I_z$ in all plots.

by the above discussion, for nominal B_1 field strength, $\omega_1/\omega_1^{nom} = 1.0$, the performance of all the pulses remains essentially perfect over the offset range $-0.1 \leqslant \Omega/\omega_1^{nom} \leqslant 0.1$. However, for field strengths much less than nominal, $\omega_1/\omega_1^{nom} \ll 1.0$, the actual offset parameter, Ω/ω_1, becomes very large and significant distortions of the profiles can be seen, especially for the passband composite pulses.

Figure 5 compares the simulated performance of broadband composite 90° and 180° pulses to the corresponding simple pulses over a larger range of resonance offsets. The simulations are shown as contour plots of the extent of excitation or inversion with the normalized B_1 field strength, ω_1/ω_1^{nom}, and the normalized resonance offset, Ω/ω_1^{nom}, on the two axes. The contour plots in Figs. 5a and 5b show the extent of absorptive excitation, $\langle I_y \rangle$, for a simple 90° pulse and the broadband composite 90° pulse $BB_1(90°)$, while Figs. 5c and 5d show the inversion, $\langle I_z \rangle$, for a simple 180° pulse and the broadband composite 180° pulse $BB_1(180°)$. This figure clearly demonstrates the point made above: the performance of the composite pulses with respect to offset is no worse over small offsets than that of the simple pulses that they are designed to replace. To show that this result is not limited to 90° and 180° pulses, Fig. 6 shows contour plots of the extent of absorptive excitation, $\langle I_y \rangle$, for (Fig. 6a) a simple 45° pulse and (Fig. 6b) a broadband composite 45° pulse $BB_1(45°)$. Again the new composite pulse exhibits an impressive bandwidth with respect to ω_1/ω_1^{nom} with little appreciable degradation of performance with respect to offset.

EXPERIMENTAL VERIFICATION

Experimental excitation and inversion profiles were measured using a Bruker MSL 400 spectrometer. The sample consisted of an aqueous solution of 2 *M* NaCl in a 5 mm outer diameter glass tube filled to a depth of 10 mm. The ^{23}Na signal was observed at a Larmor frequency of 105.8 MHz using a standard 10 mm broadband NMR probe. The choice of ^{23}Na NMR for measuring the excitation and inversion profiles was, of course, completely arbitrary: other nuclei, such as ^{1}H, ^{13}C, ^{15}N, and ^{31}P, would have given equivalent results.

The measured ^{23}Na 90° pulse length was 17.2 μs at exact resonance, $\Omega = 0$. The aim of using the small sample inside the larger coil was to minimize the true inhomogeneity of the B_1 radiofrequency field so that the effect of inhomogeneity could be mimicked by variation of the pulse flip angles. The true B_1 inhomogeneity across the sample was still sufficient, however, to distort all the experimental profiles and to make it impossible to obtain meaningful profiles by this method for the passband composite pulses (the longest of the sequences presented in this paper).

The experimental excitation profiles for (Fig. 7a) a simple 90° pulse, (Fig. 7b) the narrowband composite 90° pulse $NB_1(90°)$, (Fig. 7c) the narrowband composite 90° pulse $NB_2(90°)$, (Fig. 7d) the broadband composite 90° pulse $BB_1(90°)$, and (Fig. 7e) the broadband composite 90° pulse $BB_2(90°)$ are shown. All spectra are displayed on the same

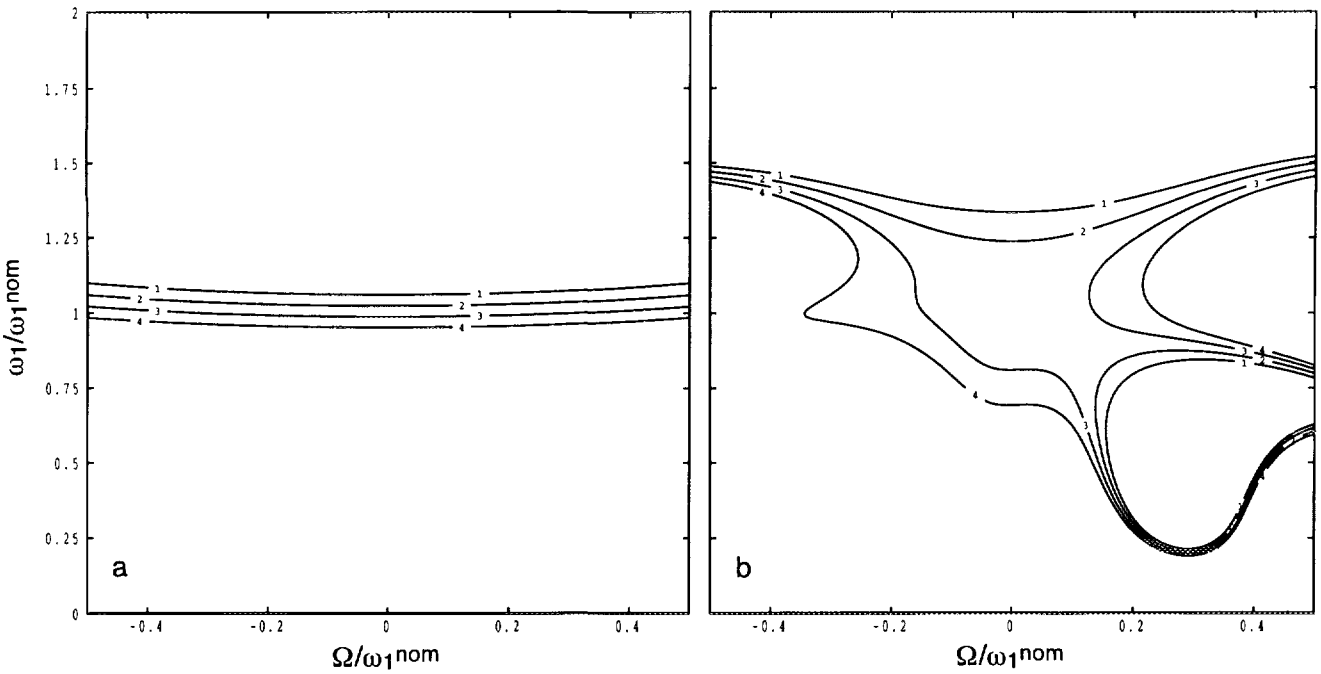

FIG. 6. Simulated contour plots of the absorptive excitation, $\langle I_y \rangle$, for (a) a simple 45° pulse and (b) a broadband composite 45° pulse $BB_1(45°)$ as a function of Ω/ω_1^{nom} and ω_1/ω_1^{nom}. Contours are drawn at (1) $\langle I_y \rangle = -0.74$, (2) -0.72, (3) -0.70, and (4) -0.68. The initial state is $\sigma(0) = I_z$ in both plots.

vertical scale. The 17 spectra in Fig. 7a were obtained by incrementing the duration of a simple pulse such that the nominal flip angle went from 10° to 170° in 10° steps as shown. The spectrum resulting from the nominal 90° pulse was phased and the same phase correction applied to the remaining 16 spectra. No other phase corrections were performed. The four series of 17 spectra in Figs. 7b–7e were obtained by an analogous approach, with the flip angles in the composite pulses incremented in concert. The theoretical profiles in Figs. 1a and 2a are confirmed. In particular, the remarkably small variation in the phase of the excited magnetization should be noted.

The experimental inversion profiles for (Fig. 8a) a simple 180° pulse, (Fig. 8b) the narrowband composite 180° pulse $NB_1(180°)$, (Fig. 8c) the narrowband composite 180° pulse $NB_2(180°)$, (Fig. 8d) the broadband composite 180° pulse $BB_1(180°)$, and (Fig. 8e) the broadband composite 180° pulse $BB_2(180°)$ are shown. Again, all spectra are displayed on the same vertical scale. The 17 spectra in Fig. 8a were obtained by incrementing the duration of a simple pulse such that the nominal flip angle went from 20° to 340° in 20° steps as shown. This "inversion" pulse was then immediately followed by a suitably phase-cycled nominal 90° pulse to monitor the extent of inversion. The four series of 17 spectra in Figs. 8b–8e were obtained by an analogous approach, with the flip angles in the composite pulses incremented in concert. The theoretical profiles in Figs. 1c and 2c are confirmed.

DISCUSSION

The most significant feature of the new composite pulses presented in this paper is that they can be used to replace a simple pulse in an advanced NMR experiment, such as a multiple-quantum filter or a multidimensional heteronuclear correlation, without further modification of the pulse sequence. In the past, composite pulses have been termed "phase distortionless" if they generate a phase shift of the magnetization that is constant and is not a function of the radiofrequency field, ω_1, or resonance offset, Ω (*9, 12*). Such a pulse can be used in advanced NMR experiments, but the phases of other pulses in the pulse sequence must be altered to compensate for the unwanted phase shift. The composite pulses presented in this paper do not generate such a phase shift and are thus much easier to implement.

Another important property of the new composite pulses is that they are available to replace simple pulses of any flip angle. These two chief virtues are best illustrated with an example. Recently, there has been much interest in the selective observation of orientationally ordered sodium ions

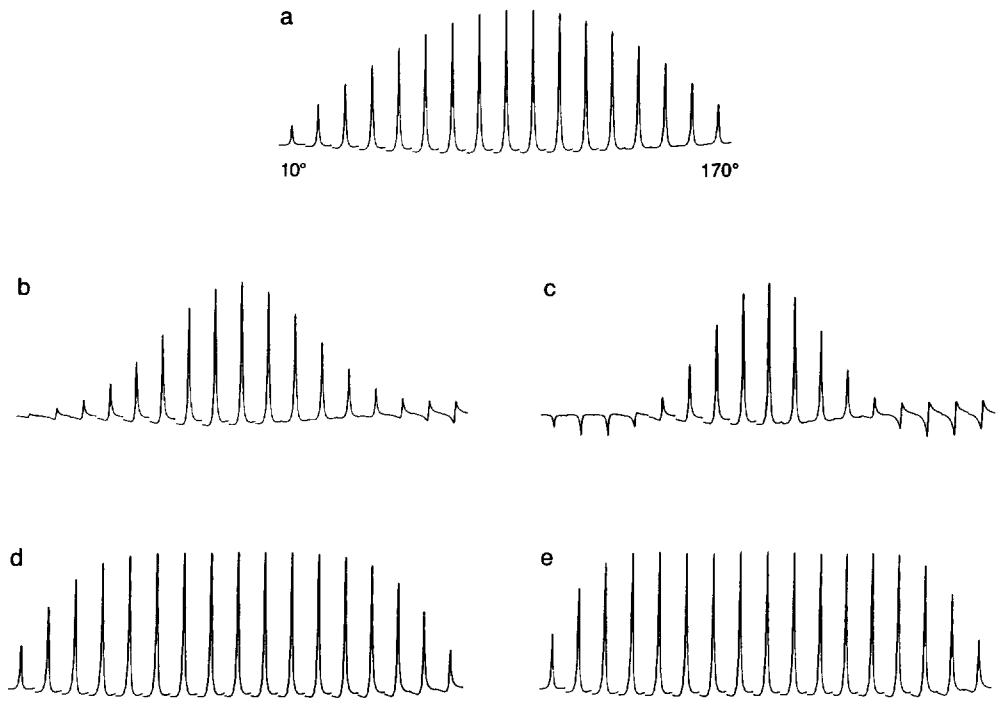

FIG. 7. Experimental excitation profiles for (a) a simple 90° pulse, (b) the narrowband composite 90° pulse $NB_1(90°)$, (c) the narrowband composite 90° pulse $NB_2(90°)$, (d) the broadband composite 90° pulse $BB_1(90°)$, and (e) the broadband composite 90° pulse $BB_2(90°)$. The 17 spectra in (a) were obtained by incrementing the duration of a simple pulse such that the nominal flip angle went from 10° to 170° in 10° steps as shown. The spectrum resulting from the nominal 90° pulse was phased and the same phase correction applied to the remaining 16 spectra. The four series of 17 spectra in (b)–(e) were obtained by an analogous approach, with the flip angles in the composite pulses incremented in concert.

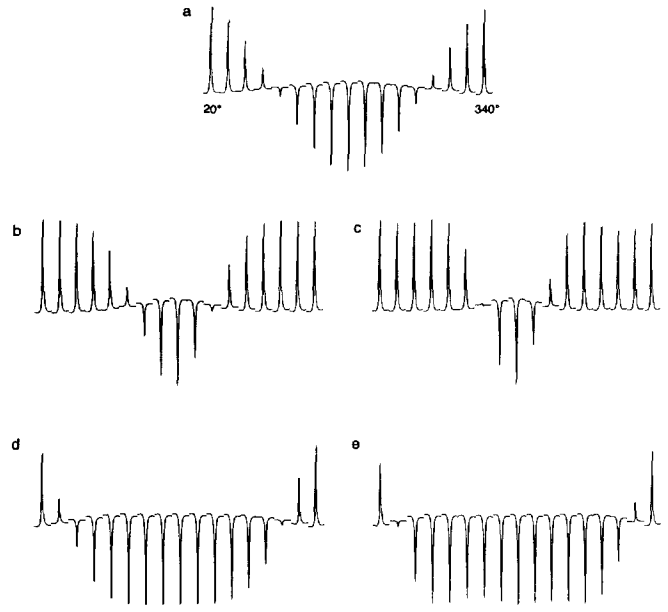

FIG. 8. Experimental inversion profiles for (a) a simple 180° pulse, (b) the narrowband composite 180° pulse $NB_1(180°)$, (c) the narrowband composite 180° pulse $NB_2(180°)$, (d) the broadband composite 180° pulse $BB_1(180°)$, and (e) the broadband composite 180° pulse $BB_2(180°)$. The 17 spectra in (a) were obtained by incrementing the duration of a simple pulse such that the nominal flip angle went from 20° to 340° in 20° steps as shown. This "inversion" pulse was then immediately followed by a suitably phase-cycled nominal 90° pulse to monitor the extent of inversion. The four series of 17 spectra in (b)–(e) were obtained by an analogous approach, with the flip angles in the composite pulses incremented in concert.

in biological systems (*22–25*). The ^{23}Na spectrum of such ions is a typically a superposition of spin-$\frac{3}{2}$ powder patterns which have been motionally narrowed to widths of 1 kHz or less. Figure 9a shows a computer simulation of a single spin-$\frac{3}{2}$ powder pattern with a maximum quadrupolar splitting of $2\nu_Q^{max}$ = 500 Hz. If the signal from sodium ions in isotropic, liquid-type environments is to be suppressed, then a pulse sequence must be used that generates only a singly antiphase spin-$\frac{3}{2}$ powder pattern (*25, 26*). One such experiment is a double-quantum filter in which the flip angles of both the pulses in the filtration step are precisely 54.7° (*22, 26*):

$$90^\circ_\phi\text{—}\tau/2\text{—}180^\circ_{\phi+90^\circ}\text{—}\tau/2\text{—}54.7^\circ_\phi\ 54.7^\circ_0\ \text{Acquire.}\quad [22]$$

The pulse phase ϕ and the receiver phase are cycled to select double-quantum coherence between the two 54.7° pulses. Figure 9b shows computer simulations of the effect of this experiment on the spin-$\frac{3}{2}$ powder pattern in Fig. 9a. If the pulses have their nominal flip angles, then an ideal singly antiphase powder pattern is produced, the absence of the intense central transition showing that no doubly antiphase component is present. In contrast, if the effect of B_1 inhomogeneity is mimicked by setting all the pulse flip angles 20% short, then there is a dramatic loss of intensity in the antiphase powder pattern and the reappearance of the (dispersive) central transition indicates the presence of a doubly antiphase component. In experimental reality, this would correspond to a considerable leakage of signal from isotropic, liquid-type sodium ions into the spectrum. However, if broadband composite pulses $BB_1(\theta)$ are used to replace all the pulses in the sequence in Eq. [22] then, even with a 20% misset in the flip angles, the loss of intensity is reversed and the central transition is again suppressed. Specifically, the 90° pulse is replaced with the broadband composite pulse $BB_1(90°) = 180^\circ_{97.2°}360^\circ_{291.5°}180^\circ_{97.2°}90^\circ_{0°}$, the 180° pulse is replaced with $BB_1(180°) = 180^\circ_{104.5°}360^\circ_{313.4°}180^\circ_{104.5°}180^\circ_{0°}$, and the 54.7° pulses are both replaced with $BB_1(54.7°) = 180^\circ_{94.4°}360^\circ_{283.1°}180^\circ_{94.4°}54.7^\circ_{0°}$.

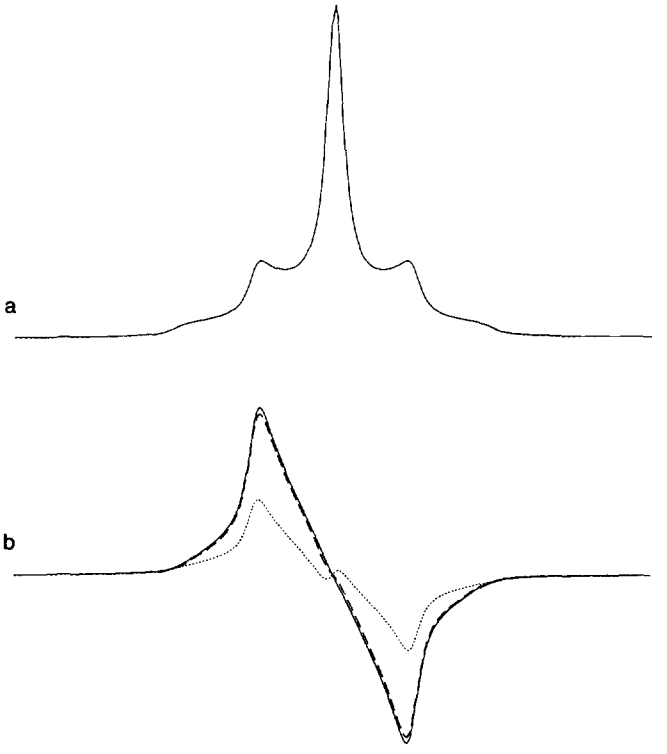

FIG. 9. Computer simulations of a spin-$\frac{3}{2}$ powder pattern, such as that shown by orientationally ordered sodium ions in biological systems. The conventional spectrum is shown in (a), while spectra produced by the double-quantum filter with 54.7° flip angles of Eq. [22] are shown in (b). If the pulses in the double-quantum filter have their nominal flip angles, then the spectrum in (b) is essentially perfect (solid line) and shows a singly antiphase spin-$\frac{3}{2}$ powder pattern. If all the pulse flip angles are set 20% short (dotted line), then the intensity of the spectrum is much reduced and a small doubly antiphase component appears (in the form of the dispersive central transition). If broadband composite pulses $BB_1(\theta)$ are used as described in the text, then, even with the flip angles 20% short (dashed line), the spectrum is restored to near perfection. Parameters used in the simulations are as follows: 5 μs 90° pulse length; $2\nu_Q^{max}$ = 500 Hz; 2 kHz spectral width; τ = 1 ms double-quantum filter evolution interval. The vertical scale in (b) is expanded by a factor of four.

When the pulse sequence or phase cycle requires, for example, a $180^{\circ}_{90^{\circ}}$ pulse, then 90° is added to the phase of all the pulses in $BB_1(180°)$, e.g., $180^{\circ}_{94.5^{\circ}}360^{\circ}_{43.4^{\circ}}180^{\circ}_{94.5^{\circ}}180^{\circ}_{90^{\circ}}$. Note that these new composite pulses are *not* broadband with respect to quadrupolar splittings and are only effective in Fig. 9 because the nutation frequency ($\omega_1/2\pi$ = 50 kHz) is much greater than the largest splitting ($2\nu_Q^{max}$ = 500 Hz).

Naturally, the new composite pulses presented in this paper do have some weaknesses. First, although their performance with respect to resonance offset is better than that of most other composite pulses of their type and seems sufficient for use in routine ^{1}H NMR spectroscopy, it is clearly a long way from being good enough for use in routine ^{13}C, ^{15}N, or ^{31}P spectroscopy, where normalized offsets of up to $\Omega/\omega_1^{nom} = \pm 1.0$ are frequently encountered. Second, some of the composite pulses require very accurate pulse phases, perhaps accurate to within 1°. These should be readily available to most spectroscopists, however, as the majority of commercial NMR spectrometers built in the past seven or eight years have a digital phase shift facility. Finally, the new composite pulse are clearly much longer than the simple pulses that they are designed to replace. For example, the composite pulse $BB_2(180°)$ is 5 times the length of a simple 180° pulse, while the passband composite pulse $PB_1(45°)$ is 33 times the length of a simple 45° pulse. Whether this increased length places a limitation on the usefulness of the composite pulse will depend on the particular application.

In summary, new broadband, narrowband, and passband composite pulses have been presented in this paper for use in situations where the B_1 radiofrequency field is inhomogeneous across the sample. They possess a unique combination of favorable properties, including (a) the absence of any unwanted phase shifts, (b) the availability of any overall flip angle, and (c) a relatively robust performance with respect to resonance offset.

ACKNOWLEDGMENTS

This work was supported in part by the Royal Society. The MSL 400 spectrometer was purchased with the aid of a grant from the Science and Engineering Research Council. I am grateful to Steven P. Brown for writing part of the computer program used for the simulations in Fig. 9.

REFERENCES

1. M. H. Levitt and R. Freeman, *J. Magn. Reson.* **33,** 473 (1979).
2. R. Freeman, S. P. Kempsell, and M. H. Levitt, *J. Magn. Reson.* **38,** 453 (1980).
3. M. H. Levitt, *J. Magn. Reson.* **48,** 234 (1982).
4. R. Tycko, *Phys. Rev. Lett.* **51,** 775 (1983).
5. M. H. Levitt and R. R. Ernst, *J. Magn. Reson.* **55,** 247 (1983).
6. A. J. Shaka and R. Freeman, *J. Magn. Reson.* **55,** 487 (1983).
7. R. Tycko and A. Pines, *Chem. Phys. Lett.* **111,** 462 (1984).
8. A. J. Shaka and R. Freeman, *J. Magn. Reson.* **59,** 169 (1984).
9. R. Tycko, H. M. Cho, E. Schneider, and A. Pines, *J. Magn. Reson.* **61,** 90 (1985).
10. R. Tycko, A. Pines, and J. Guckenheimer, *J. Chem. Phys.* **83,** 2775 (1985).
11. H. M. Cho, R. Tycko, A. Pines, and J. Guckenheimer, *Phys. Rev. Lett.* **56,** 1905 (1986).
12. M. H. Levitt, *Prog. NMR Spectrosc.* **18,** 61 (1986).
13. H. Cho, J. Baum, and A. Pines, *J. Chem. Phys.* **86,** 3089 (1987).
14. H. Cho and A. Pines, *J. Chem. Phys.* **86,** 6591 (1987).
15. S. Wimperis, *J. Magn. Reson.* **83,** 509 (1989).
16. S. Wimperis, *J. Magn. Reson.* **86,** 46 (1990).
17. R. Tycko, *Adv. Magn. Reson.* **15,** 1 (1990).
18. S. Wimperis, *J. Magn. Reson.* **93,** 199 (1991).
19. R. Tycko and A. Pines, *J. Magn. Reson.* **60,** 156 (1984).
20. A. J. Shaka, J. Keeler, M. B. Smith, and R. Freeman, *J. Magn. Reson.* **61,** 175 (1985).
21. A. J. Shaka and A. Pines, *J. Magn. Reson.* **71,** 495 (1987).
22. U. Eliav, H. Shinar, and G. Navon, *J. Magn. Reson.* **98,** 223 (1992).
23. H. Shinar, T. Knubovets, U. Eliav, and G. Navon, *Biophys. J.* **64,** 1273 (1993).
24. J. S. Tauskela and E. A. Shoubridge, *Biochim. Biophys. Acta* **1158,** 155 (1993).
25. R. Kemp-Harper and S. Wimperis, *J. Magn. Reson. B* **102,** 326 (1993).
26. G. Jaccard, S. Wimperis, and G. Bodenhausen, *J. Chem. Phys.* **85,** 6282 (1986).